

SYNCHRONIZATION OF TWO-ROTOR VIBRATION UNITS USING NEURAL NETWORK-BASED PID CONTROLLER

Hoang Duc Long

Control Systems and Robotics
ITMO University
Russia
longhd@mta.edu.vn

Natalia Dudarenko

Control Systems and Robotics
ITMO University
Russia
dudarenko@yandex.ru

Article history:

Received 14.12.2021, Accepted 25.09.2022

Abstract

In the paper, the problem of controlled synchronization of Two-rotor Vibration Units is considered. A new bidirectional control law combined with Neural Network based PID controller is proposed for multi-synchronization of rotors. Besides, an algorithm for constructing Neural Network based PID Controller of Two-rotor Vibration Units is developed. The robustness of the proposed controller under the effect of unknown exogenous disturbances is illustrated.

Key words

Synchronization, Two-rotor Vibration Units, Neural Network, PID Controller, Phase shift, Vibration machine, robustness.

1 Introduction

Vibration systems using two rotors are widely used in technical systems, such as aircraft, vehicles, and industrial machines [Jörn et al., 2013, Richard et al., 2020, Xin et al., 2016, Liu et al., 2020, Zhang et al., 2017]. They are used to increase productivity or solve the problem of ensuring the stable velocity of motors. The feasibility of the applications of the Two-rotor Vibration Units for the control vibration systems was investigated [Richard et al., 2014, Nan Zhang and Shiling Wu, 2020, Li et al., 2020]. In these papers, the authors built the mathematical model of Two-rotor systems and studied possibilities for synchronous velocity between two vibration actuators.

The definition of self-synchronization and controlled synchronization of systems was presented in the paper [Fradkov et al., 1997], and the techniques of Multi-motor Synchronization were proposed in the paper [Perez-Pinal et al., 2004]. Based on two papers, there were many studies about the bidirectional controlled phase

shift and speed of unbalanced rotors [Fradkov et al., 2002, Fradkov et al., 2005, Kudryavtseva and Tomchina, 2009, Belov et al., 2017, Fradkov et al., 2021, Andrievsky and Boikov, 2021]. In the studies [Fradkov et al., 2002, Fradkov et al., 2005, Kudryavtseva and Tomchina, 2009, Belov et al., 2017], the authors built the dynamical model of the controlled plant and designed the control algorithms based on the speed-gradient method. However, the authors did not mention the behavior of the system under the effect of disturbances. In the studies [Fradkov et al., 2021, Andrievsky and Boikov, 2021], the authors used the three PI-controllers for Two-vibration Units in which one PI-controller for phase difference and two PI-controllers for two rotors. However, the PI-controllers do not keep the stability of the system under the effect of disturbances and it is difficult to define the coefficients of the PI-controllers.

There are many methods to find the coefficients of PID controller such as Fuzzy Logic Control [Malleham and Rajani, 2006], Genetic Algorithm [Zhao and Xi, 2020], and Neural Network [Jacob and Murugan, 2016, Saad, 2013, Kumarl et al., 2016, Slama et al., 2019]. An artificial neural network can be used for tuning the PID controller and is robust with disturbances [Jacob and Murugan, 2016, Saad, 2013, Kumarl et al., 2016, Slama et al., 2019]. However, the use of Neural Network based PID controller for Two-rotor Vibration Units to control the phase shift and speed is not found in the resources before here. In this paper, the authors used the Neural Network based PID controller for Two-rotor Vibration Units to control the phase shift and velocity of two motors. The simulation results of the proposed controller for frequency stabilization of the rotation angular velocities at the desired level along with reaching the prescribed phase shift between the rotor angles are demonstrated. Finally, a comparison between the new controller and PID Controller has been performed.

The paper is organized as follows. The problem formulation of phase shift control and the related problem of control of vibrational fields for is given in Section 2. In Section 3, the Nonlinear Autoregressive-Moving Average (NARMA-L2) Model which is used to tune the coefficients of PID controller is described. The Neural Network based PID Controller is proposed to solve the problems of the phase Shift and Speed-Synchronization. In Section 4, the proposed method is applied to control Two-rotor Vibration Units with the desired phase shift and desired Speed of two motors. The simulation results confirming the performance of the proposed controller are also demonstrated. Concluding remarks and discussion of future work are presented in Section 5.

2 Problem formulation

The Two-rotor Vibration Units consist of two unbalanced rotors driven by two DC motors and mounted on a supporting body that is connected to a solid base by means of an elastic element with stiffness c_0 , and a linear damper with damping coefficient β . Assume that the shafts of rotors are orthogonal to the motion of the supporting body and consider the only vertical motion of the system (Figure 1). The mathematical model of the sys-

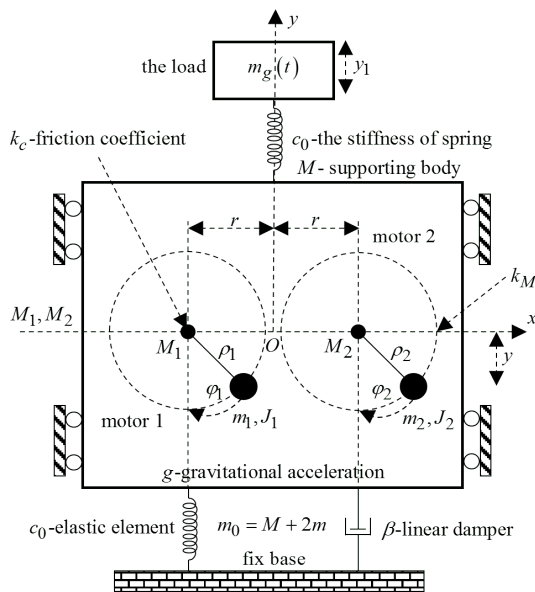


Figure 1. Two-Rotor Vibration Units

tem can be described by the model below [Kudryavtseva and Tomchina, 2009].

$$\begin{cases} m_0 \ddot{y} + m_1 \rho_1 \sin \varphi_1 \cdot \ddot{\varphi}_1 + m_2 \rho_2 \sin \varphi_2 \cdot \ddot{\varphi}_2 \\ + m_1 \rho_1 \cos \varphi_1 \cdot \dot{\varphi}_1^2 + m_2 \rho_2 \cos \varphi_2 \cdot \dot{\varphi}_2^2 \\ + c_0 y + c_1 (y - y_1) + m_0 g + \beta \dot{y} = 0 \\ J_1 \ddot{\varphi}_1 + (\ddot{y} + g) m_1 \rho_1 \sin \varphi_1 + k_c \dot{\varphi}_1 = M_1 \\ J_2 \ddot{\varphi}_2 + (\ddot{y} + g) m_2 \rho_2 \sin \varphi_2 + k_c \dot{\varphi}_2 = M_2 \\ m_g(t) (\ddot{y}_1 + g) + c_1 (y_1 - y) \\ + \dot{m}_g(t) \dot{y}_1 = 0 \end{cases} \quad (1)$$

where ϕ_1, ϕ_2 are rotation angles of the rotors measured from the lowest vertical position; y is the vertical displacement of the supporting body from the equilibrium position; y_1 is the vertical displacement of the load from the equilibrium position; m_1, m_2, M are the masses of the rotors and the supporting body, respectively; $m_g(t)$ is the weight of load; J_1, J_2 are the inertia moments of the rotors; p_1, p_2 are the eccentricities of rotors; k_c is the friction coefficient in the bearings; β is the viscous friction coefficient of the damper; c_0, c_1 are the spring stiffness; k_M is a motor parameter; $m_0 = M + 2m$; g is the gravitational acceleration; M_1 and M_2 are the magnetic torques of motors.

The schematic diagram of an armature controlled DC motor is showed in Figure 2.

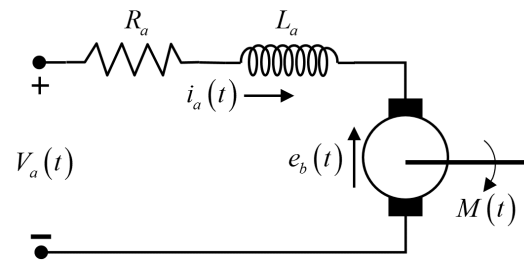


Figure 2. Schematic diagram of an armature controlled DC motor

According to the voltage balance relation between the circuit loops, the motor equation is obtained as below

$$V_a(t) = R_a i_a(t) + L_a \frac{di_a(t)}{dt} + e_b(t) \quad (2)$$

where $V_a(t)$ is the applied armature voltage; $i_a(t)$ is the armature current; $e_b(t)$ is the back emf; R_a is armature winding resistance; L_a is armature winding inductance. The back emf is proportional to speed

$$e_b(t) = K_e \dot{\varphi}(t) \quad (3)$$

where K_e is the back emf constant. The torque developed by the motor is proportional to the armature current

$$M(t) = K_t i_a(t) \quad (4)$$

where K_t is the motor torque constant.

The total inductance value L_a is very small ($L_a \ll$), so L_a can be neglected in the calculations. From equations (1), (2) and (3), the magnetic torque of motor is written in the form

$$M(t) = \frac{K_t}{R_a} \{V_a(t) - K_e \dot{\varphi}(t)\} \quad (5)$$

From equations (1) and (5), the mathematical model of Two-rotor Vibration Units has the form

$$\left\{ \begin{array}{l} m_0 \ddot{y} + m_1 \rho_1 \sin \varphi_1 \cdot \ddot{\varphi}_1 + m_2 \rho_2 \sin \varphi_2 \cdot \ddot{\varphi}_2 \\ + m_1 \rho_1 \cos \varphi_1 \cdot \dot{\varphi}_1^2 + m_2 \rho_2 \cos \varphi_2 \cdot \dot{\varphi}_2^2 \\ + c_0 y + c_1 (y - y_1) + m_0 g + \beta \dot{y} = 0 \\ J_1 \ddot{\varphi}_1 + (\dot{y} + g) \cdot m_1 \rho_1 \sin \varphi_1 + k_c \dot{\varphi}_1 \\ = \frac{K_t}{R_a} \{V_1(t) - K_e \dot{\varphi}_1\} \\ J_2 \ddot{\varphi}_2 + (\dot{y} + g) \cdot m_2 \rho_2 \sin \varphi_2 + k_c \dot{\varphi}_2 \\ = \frac{K_t}{R_a} \{V_2(t) - K_e \dot{\varphi}_2\} \\ m_g(t) (\dot{y}_1 + g) + c_1 (y_1 - y) \\ + \dot{m}_g(t) \dot{y}_1 = 0 \end{array} \right. \quad (6)$$

where $V_1(t)$ and $V_2(t)$ are the armature voltages of motors (control variables).

In a number of important cases, the synchronous rotational mode with the desired steady-state value of the phases is stable due to the self-synchronization phenomenon. However, it is necessary to provide either an alternative stable phase shift of the rotors or to increase the robustness of the existing phase shift. In both cases, the problem of controlled synchronization is worth to be posed.

3 Control design method

3.1 The Nonlinear Auto-regressive Moving Average (NARMA-L2) Model

The NARMA-L2 model is one of the most widely used models for time series forecasting [Haider et al., 2019, Jibril et al., 2020, Humod et al., 2016]. In this paper, the authors use the NARMA-L2 model to find the coefficients of PID controller. The first step in using feedback linearization (or NARMA-L2 control) is to identify the system to be controlled. The first step is to choose a model structure. One standard model that has been used to represent general discrete-time nonlinear systems is the Nonlinear Autoregressive-Moving Average (NARMA-L2) model:

$$y(k+d) = N \left(\begin{array}{l} y(k), y(k-1), \dots, \\ y(k-n+1), \\ u(k), u(k-1), \dots, \\ u(k-n+1) \end{array} \right) \quad (7)$$

where $u(k)$ is the system input, and $y(k)$ is the system output. For the identification phase, the nonlinear function N could be approximated by a trained neural network. This is the identification procedure used for the NN Predictive Controller. To the system output following some reference trajectory $y(k+d) = y_r(k+d)$, the next step is to develop a nonlinear controller of the form:

$$u(k) = G \left(\begin{array}{l} y(k), y(k-1), \dots, \\ y(k-n+1), y_r(k+d), \\ u(k-1), \dots, u(k-m+1) \end{array} \right) \quad (8)$$

To use this controller, the dynamic backpropagation (the outputs of system, the former inputs and reference trajectory are the inputs of the neural network) is used to train a neural network to create the function G that will minimize mean square error. This can be quite slow. One solution is to use approximate models to represent the system. The controller used in this section is based on the NARMA-L2 approximate model:

$$\hat{y}(k+d) = f \left(\begin{array}{l} y(k), y(k-1), \dots, \\ y(k-n+1), u(k-1), \\ \dots, u(k-m+1) \end{array} \right) + g \left(\begin{array}{l} y(k), y(k-1), \dots, \\ y(k-n+1), u(k-1), \\ \dots, u(k-m+1) \end{array} \right) u(k) \quad (9)$$

This model is in companion form, where the next controller input $u(k)$ is not contained inside the nonlinearity. This form can be used to solve for the control input that causes the system output to follow the reference $y(k+d) = y_r(k+d)$. The resulting controller would have the form

$$u(k) = \frac{y_r(k+d) - f \left(\begin{array}{l} y(k), \\ y(k-1), \dots, \\ y(k-n+1), \\ u(k-1), \dots, \\ u(k-n+1) \end{array} \right)}{g \left(\begin{array}{l} y(k), \\ y(k-1), \dots, \\ y(k-n+1), \\ u(k-1), \dots, \\ u(k-n+1) \end{array} \right)} \quad (10)$$

Using this equation directly can cause realization problems, because the control input $u(k)$ must be determined that based on the output at the same time, $y(k)$. So, instead, use the model

$$y(k+d) = f \left(\begin{array}{l} y(k), y(k-1), \dots, \\ y(k-n+1), u(k), \\ u(k-1), \dots, \\ u(k-n+1) \end{array} \right) + g \left(\begin{array}{l} y(k), \dots, y(k-n+1), \\ u(k), \dots, u(k-n+1) \end{array} \right) u(k+1) \quad (11)$$

where $d \geq 2$. Figure 3 shows the structure of a neural network representation. In this Figure, The tapped delay line (TDL) makes full use of the linear network. There the input signal enters from the left and passes through $N-1$ delays. The output of the tapped delay line is an N -dimensional vector, made up of the input signal at the current time, the previous input signal, etc.

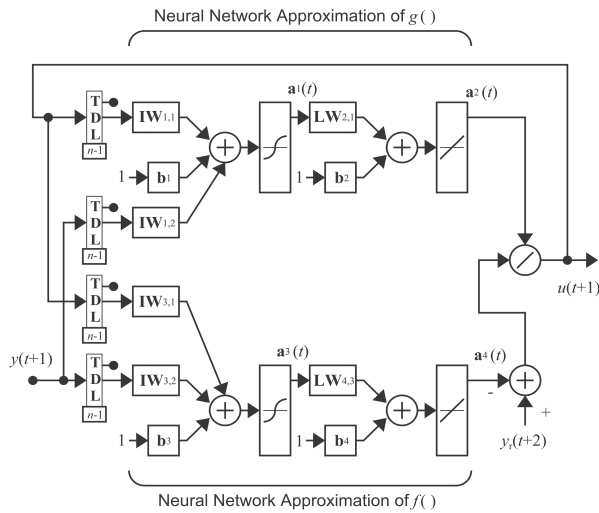


Figure 5. The implementation of the NARMA-L2 controller

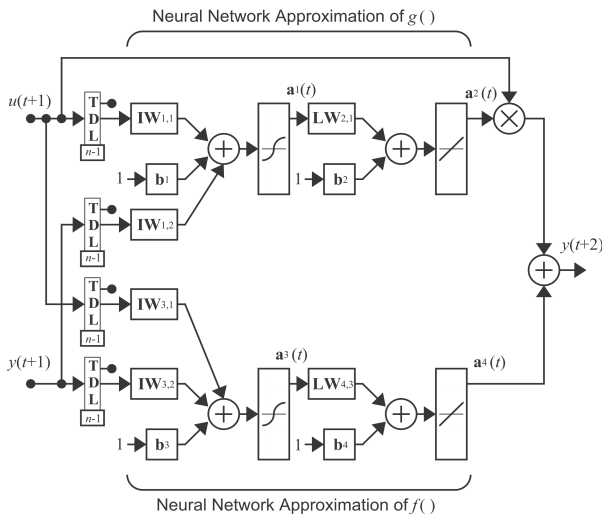


Figure 3. The block diagram of NARMA-L2 Model Identification

Using the NARMA-L2 model, the controller can be obtained

$$u(k+1) = \frac{y_r(k+d) - f \begin{pmatrix} y(k), \dots, y(k-n+1) \\ u(k), \dots, u(k-n+1) \end{pmatrix}}{g \begin{pmatrix} y(k), \dots, y(k-n+1) \\ u(k), \dots, u(k-n+1) \end{pmatrix}} \quad (12)$$

which is realizable for $d \geq 2$. The block diagram of the NARMA-L2 Controller as Figure 4.

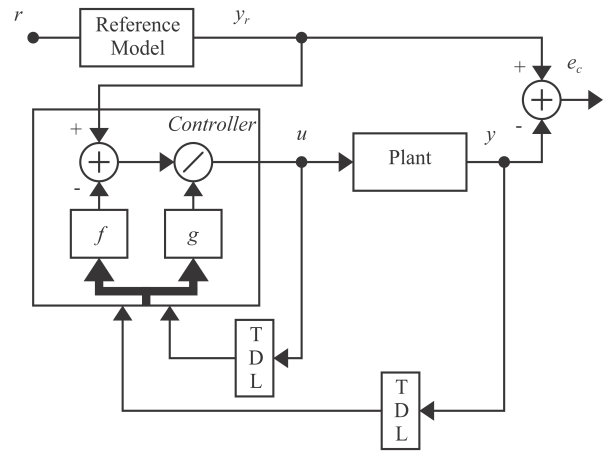


Figure 4. The block diagram of the NARMA-L2 controller

This controller can be implemented with the previously identified NARMA-L2 plant model, as shown in the following Figure 5.

3.2 Neural Network based PID Controller

Proportional Integral Derivative (PID) controllers are the most used controllers in industrial control systems. There is the well-known Ziegler-Nichols method [Malle-sham and Rajani, 2006, Saad, 2013] to tune the coefficients of the PID controller. This tuning method is simple and gives fixed values for the coefficients which make the PID controller have weak adaptabilities for the model parameters variation and changing in operating conditions. However, in the case of white noise affected on the system, the Ziegler-Nichols method is difficult to find exactly the coefficients of PID controller. In order to achieve an adaptive controller, the Neural Network (NN) control combines the PID controller to guarantee the desired qualities of the system. There are some studies using the Neural Network to find coefficients of PID Controller [Jacob and Murugan, 2016]. The typical model of Neural Network combines PID Controller is illustrated in Figure 6. Figure 6 shows that the NARMA-L2 Controller was used to find the coefficient of PID Controller. The NARMA-L2 Controller has two input (Reference and Plant Output) and one output (Control Signal).

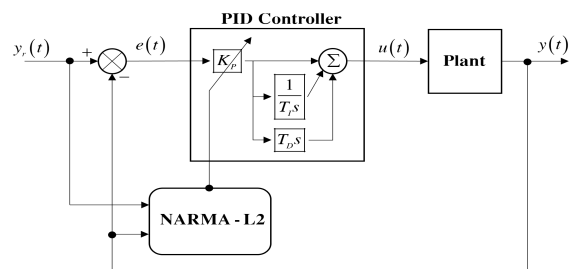


Figure 6. The general model of Neural Network based PID Controller

The block diagram of Two-rotor Vibration Units using

the NARMA-L2 Controller to find the coefficients of the PID Controller is illustrated in Figure 7. Besides, Figure 7 also illustrates the control algorithm in section (3.3). The disturbances are put on the shafts of motors. The NARMA-L2 Controller is used to evaluate the effects of the disturbances on the shafts of two rotors that affect the phase shift and calculate the coefficients of PID Controllers.

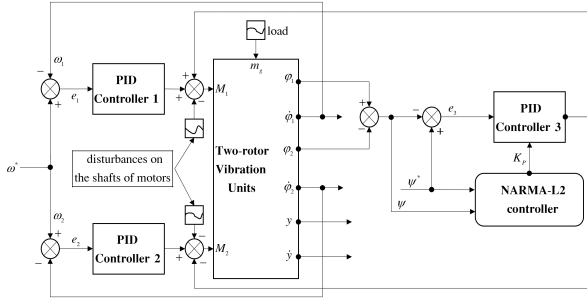


Figure 7. The general model of Neural Network based PID Controller

3.3 Control algorithm of Two-rotor Vibration Units using Neural Network based PID Controller

The authors designed the control algorithms ensuring the prescribed phase shift $\psi = \varphi_l - \varphi_r$ between the unbalanced rotor rotation angles φ_l and φ_r simultaneously with the given rotation speed $\omega_l = \omega_r = \omega^*$.

Algorithm for constructing Neural Network based PID Controller of Two-rotor Vibration Units consists of 4 steps:

Step 1. Build the mathematic model (1) of Two-rotor Vibration Units using Euler-Lagrange equation

$$\frac{d}{dt} \left(\frac{\partial L}{\partial \dot{q}_i} \right) - \frac{\partial L}{\partial q_i} = 0 \quad (13)$$

where L is the sum of kinetic energy and potential energy of system; q_i is the state variable.

Step 2. Use two PID Controllers to control the desired velocity of two motors

$$\text{PID}_{\omega} \text{controller} : \begin{cases} e_{l,r}(t) = \omega_{l,r}^*(t) - \omega_{l,r}(t) \\ u_{\omega_{l,r}}(t) = k_{P_{\omega}} e_{l,r}(t) \\ + k_{I_{\omega}} \int e_{l,r}(t) dt \\ + k_{D_{\omega}} \frac{de_{l,r}(t)}{dt} \end{cases} \quad (14)$$

where $\omega_{l,r}^*(t)$ are the reference angular velocities for left l and right r rotors, respectively; $\omega_{l,r}(t)$ are the corresponding current values of the angular rotation velocities (rad/s); $u_{\omega_{l,r}}(t)$ are the dimensionless control signals for the corresponding motor; $k_{P_{\omega}}, k_{I_{\omega}}, k_{D_{\omega}}$ are the proportional and integral controller gains.

Step 3. Calculate the phase shift of two motors and use

a PID Controller to compensate the energy for two PID Controller in the step (2)

$$\text{PID}_{\psi} \text{controller} : \begin{cases} \psi(t) = \varphi_l(t) - \varphi_r(t) \\ \Delta\psi(t) = \psi^* - \psi(t) \\ u_{\psi}(t) = k_{P_{\psi}} \Delta\psi(t) \\ + k_{I_{\psi}} \int \Delta\psi(t) dt \\ + k_{D_{\psi}} \frac{d\Delta\psi(t)}{dt} \end{cases} \quad (15)$$

where ψ^* is the desired phase shift; $k_{P_{\psi}}, k_{I_{\psi}}, k_{D_{\psi}}$ are the proportional and integral controller gains.

For the considered case of two rotors, this leads to adding synchronization signal $u_{\psi}(t)$ to the frequency controls with the opposite signs to the left and the right drives as follows:

$$\begin{cases} u_l(t) = u_{\omega_l}(t) - u_{\psi}(t) \\ u_r(t) = u_{\omega_r}(t) + u_{\psi}(t) \end{cases} \quad (16)$$

Step 4. Use the NARMA-L2 as equation (7) to update exactly the coefficients of PID Controllers when the system is affected by disturbances.

4 The Results of Computer Simulation

The study of Neural Network based PID Controller was carried out using computer simulation in the MATLAB environment for Two-rotor Vibration Unit, shown in Figure 8. In the example, the authors use a Neural Network based PID Controller for the phase shift of two motors to prove the quality of proposed controller. During the simulation, the parameters of the system were set: $M = 9(\text{kg})$; $m_1 = m_2 = 1.5(\text{kg})$; $p_1 = p_2 = 0.04(\text{m})$; $g = 9.81(\text{kg.m/s}^2)$; $c_0 = 5300(\text{kg.m}^2/\text{s})$; $k_e = 0.01(\text{kg.m}^2/\text{s})$; $b = 5(\text{kg.m}^2/\text{c})$; $J_1 = J_2 = 0.014(\text{kg.m}^2)$; $K_e = 0.06(\text{V.s/rad})$; $K_t = 0.06(\text{N.m/A})$; $R_a = 1.2(\text{ohms})$.

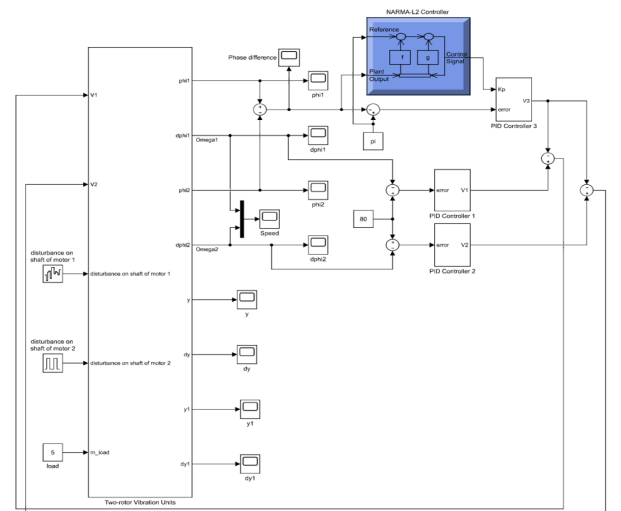


Figure 8. The diagram of Two-rotor Vibration Unit using Neural Network based PID Controller

NARMA-L2 Controller is set on Simulink of MATLAB as Figure 9. The authors used the "cstr" Simulink model to generate training data, which consists one input (the phase shift $\psi(t) = \varphi_l(t) - \varphi_r(t)$) and one output (K_P -coefficient of PID controller). The criterion for the quality of training of the neural network inside the NARMA-L2 controller is the minimum of mean squared error between the reference and plant output. Size of Hidden Layer (the number of neurons in the first layer of the plant model network) and Training Epochs (Number of iterations of plant training to be performed) are chosen based on the property of NARMA-L2 controller and the property of Two-rotor Vibration Units system. In the simulation, the authors chose the Size of Hidden Layer is 100, the Training Samples is 800 and the Training Epochs is 200.

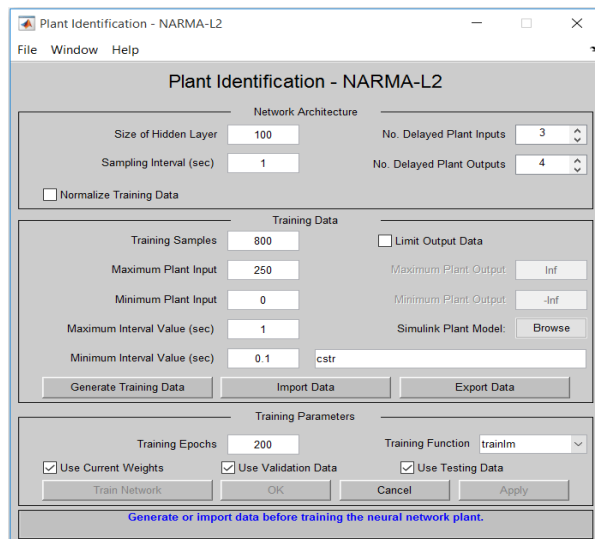


Figure 9. The setting of NARMA-L2 Controller

The authors conducted the comparison in the proposed controller and PID Controller. Figure 10 showed the two controller in the case system without disturbances. The setting time of Neural Network-based PID Controller is smaller than the setting time of PID Controller (see Figure 10(a)) and there is no error of rotors' speed in the case of Neural Network-based PID Controller while the velocities of rotors have resonance values in the case of PID Controller (see Figure 10(c,d)). The vertical displacement of the supporting body are the same with two controllers (see Figure 10(b)). The controlling voltages V_1 and V_2 to approach the desired value are shown in Figure 10(e,f).

Figure 11 showed the two controllers in the case system with disturbances on the shafts of two rotors: The white noise (noise power=50 and sample time=1s) affected on the shaft of motor 1 and the harmonic disturbance (amplitude=50 and period=1s) affected on the shaft of motor 2. The phase shift and motors' speed of the case PID

Controller are unstable (see Figure 11(a)). The vertical displacement of the supporting body are higher with PID controllers (see Figure 11(b)). The velocities of rotors have high resonance values in the case of PID Controller (see Figure 11(d)). The controlling voltages V_1 and V_2 to approach the desired value are shown in Figure 11(e,f). When the load is changed as the Ramp function (slope=1 and initial output=0.2), the behavior of the system is performed in Figure 12. Figure 12(a) shows the phase difference is unstable at desired value with the PID controller while still good adapt with the proposed controller. In Figure 12(b), as the load increases with the ramp function, the displacement of the supporting body in the case of the PID controller is larger and more oscillated than in the case of the proposed controller. Figure 12(c,d) shows the effects of changed load on the rotors' speed. In addition, the rotors' speed deviated strongly from the desired value in the case of the PID controller while the rotors' speed did not change in the case of the Neural Network based PID controller. The controlling voltages V_1 and V_2 to approach the desired value are shown in Figure 12(e,f).

5 Conclusion

In the paper, the problems of Phase Shift and Speed-synchronization are solved by using Neural Network based PID Controller. The comparison of the output of the proposed controller with PID Controller proves the effectiveness of the Neural Network based PID Controller.

In the future, the authors focus on the movement of vibrating platforms due to multiple synchronization with a controlled phase shift and use the NARMA-L2 Controller for finding coefficients of PID Controllers of two motors to enhance the quality of the system under any exogenous disturbances.

References

- Boris Andrievsky, Vladimir I. Boikov (2021). Bidirectional controlled multiple synchronization of unbalanced rotors and its experimental evaluation. *Cybernetics and Physics*, Volume 10, No.2, pp. 63–74.
- Ph. A. Belov, D. V. Gorlatov, O. P. Tomchina (2017). Complex of models of multi-rotor vibration units: From the model to the experiment (Russian). *Informatics and control systems*, No.2(52), 2017, pp.25-36.
- H. Nijmeijer, I.L. Blekhman, A.L. Fradkov, A.Yu. Pogromsky (1997). Self-synchronization and controlled synchronization. *1st International Conference, Control of Oscillations and Chaos Proceedings*, St. Petersburg, Russia, pp.36-41.
- I.I. Blekhman, A.L. Fradkov, O.P. Tomchina and D.E. Bogdanov (2002). Self-synchronization and controlled synchronization: general definition and example design. *Mathematics and Computers in Simulation (MATCOM)*, Volume 58, Issue 4, pp.367-384.

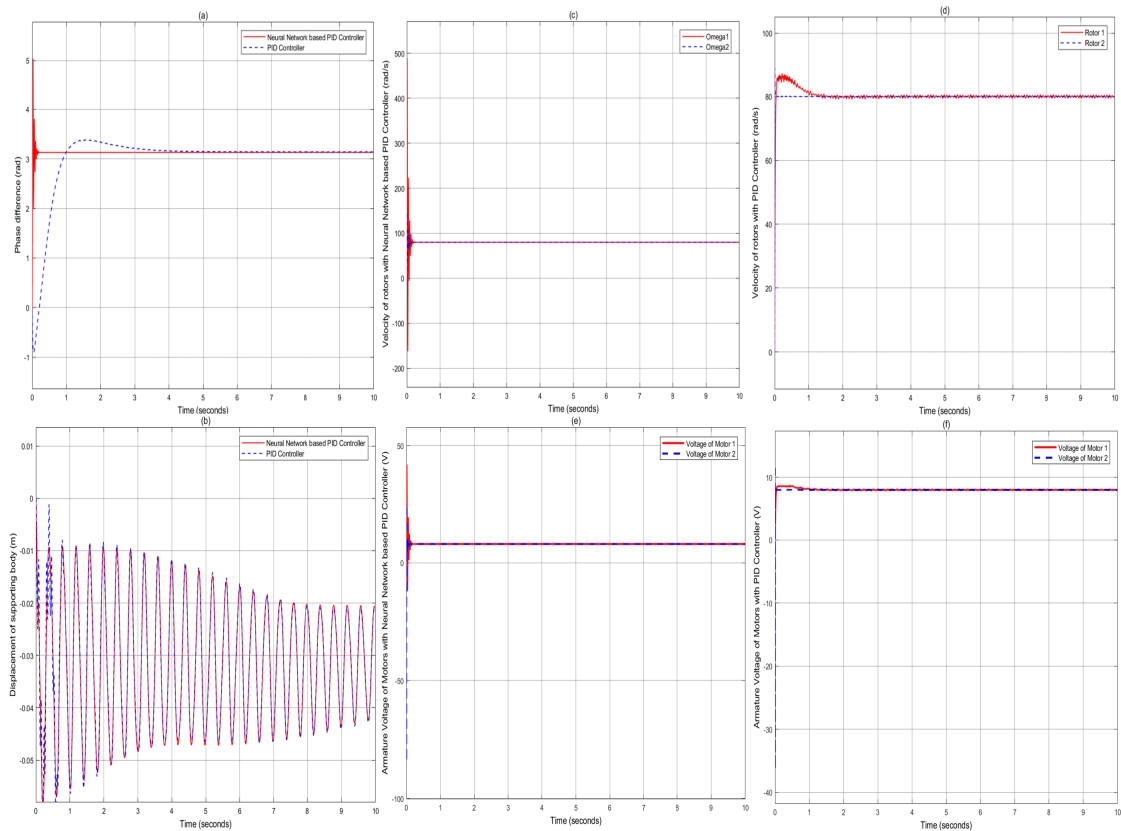


Figure 10. The response of system with Neural Network based PID Controller and PID Controller without disturbances.

- Fradkov, A., Andrievsky, B., Boykov, K. (2005). Control of the coupled double pendulums system. *Mechatronics*, Volume 15, Issue 10, pp.1289-1303, <https://doi.org/10.1016/j.mechatronics.2005.03.008>.
- Alexander L. Fradkov, Olga P. Tomchina, Boris Andrievsky, Vladimir I. Boikov (2021). Control of Phase Shift in Two-Rotor Vibration Units. *IEEE Transactions on Control Systems Technology*, Volume 29, Issue 3, May 2021, pp.1316-1323, DOI:10.1109/TCST.2020.2983353.
- A. Haider, S.A. Al-Mawsawi, Q. Alfaris (2019). Nonlinear Auto-Regressive Moving Average (NARMA-L2) Controller Design for UPFC. *WSEAS Transactions on Electronics*, Volume 10, pp.101-108.
- Abdulrahim T. Humod, Ali H. Almukhtar, Huda B. Ahmed (2016). Direct Torque Control for Permanent Magnet Synchronous Motor Based on NAR-MA-L2 controller. *Engineering and Technology Journal*, Volume 34, Part (A), No.3, 2016, pp.464-482.
- Rosmin Jacob, Senthil Murugan (2016). Implementation of neural network based PID controller. *International Conference on Electrical, Electronics, and Optimization Techniques*, pp.2769-2771.
- Mustefa Jibril, Eliyas Alemayehu Tadese, Abu Fayo (2020). Nonlinear Auto-Regressive Moving Average-L2 Model Based Adaptive Control of Nonlinear ARM Nerve Simulator System. *International Research Journal of Modernization in Engineering Technology and Science*, Volume 02, Issue:03, March 2020, pp.159-171.
- Jörn SCHELLER, Uwe STAROSSEK (2013). Twin Rotor Damper for Control of Wind-Induced Bridge Deck Vibrations. *15th Asia Pacific Vibration Conference*, 2-6 June 2013, pp.347-352.
- I.M. Kudryavtseva, O. P. Tomchina (2009). Algorithm of multiple synchronization for a two-rotor vibration stand with a non-stationary load (Russian). *Cybernetic Physics 2009*, No.3(21), pp.34-44.
- Rajesh Kumarl, Smriti Srivastava, J.R.P. Gupta (2016). Artificial Neural Network based PID Controller for Online Control of Dynamical Systems. *1st IEEE International Conference on Power Electronics, Intelligent Control and Energy Systems (ICPEICES-2016)*.
- Yujia Li, Tao Ren, Xiaoping Meng, Minghong Zhang, Peng Zhao (2020). Experimental and theoretical investigation on synchronization of a vibration system flexibly driven by two motors. *Proceedings of the Institution of Mechanical Engineers, Part C: Journal of Mechanical Engineering Science*, Volume 234, Issue 13, <https://doi.org/10.1177/0954406220907930>.
- Yunshan Liu, Xueliang Zhang, Dawei Gu, Lei Jia, Bangchun Wen (2020). Synchronization of a Dual-Mass Vibrating System with Two Exciters. *Shock and Vibration*, Volume 2020, Article ID 9345652, 12 pages, <https://doi.org/10.1155/2020/9345652>.
- Gaddam Malleshham, Akula Rajani (2006). Automatic

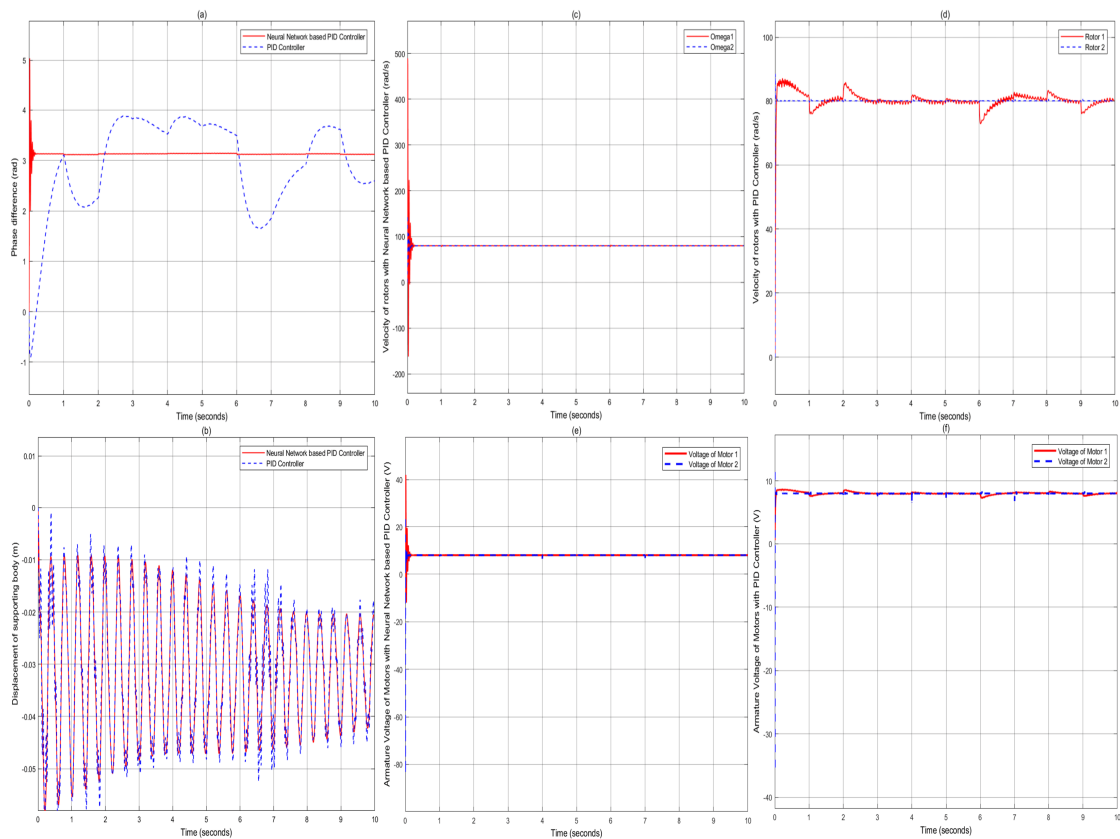


Figure 11. The response of system with Neural Network based PID Controller and PID Controller with disturbances on the shafts of two rotors.

tuning of PID Controller using Fuzzy Logic. *8th International Conference on Development and Application Systems*, Suceava, Romania, pp.120-127.

Perez-Pinal, C. Nunez, R. Alvarez, I. Cervantes (2004). Comparison of Multi-motor Synchronization Techniques. *30th Annual Conference of IEEE Industrial Electronics Society*, Busan, Korea, pp.1670-1675.

Richard Bäumer, Uwe Starossek, Jörn Scheller (2014). Continuous state feedback control for twin rotor damper. *Proceedings of the 9th International Conference on Structural Dynamics*, EURO-DYN 2014, Porto, Portugal, 30 June - 2 July 2014, pp.1647-1654.

Richard Terrill, Richard Bäumer, Katrien Van Nimmen, Peter Van den Broeck, Uwe Starossek (2020). Twin Rotor Damper for Human-Induced Vibrations of Footbridges. *Journal of Structural Engineering*, Volume 146, Issue 7.

Saad Zaghlul Saeed Al-Khayyt (2013). Tuning PID Controller by Neural Network for Robot Manipulator Trajectory Tracking. *Al-Khwarizmi Engineering Journal*, Volume 8, No.1, pp.19-28.

Sabrina Slama, Ayachi Errachdi, Mohamed Benrejeb (2019). Neural Adaptive PID and Neural Indirect Adaptive Control Switch Controller for Nonlinear

MIMO Systems. *Mathematical Problems in Engineering*, Volume 2019, Article ID 7340392, 11 pages, <https://doi.org/10.1155/2019/7340392>.

Xin Lai, Wanjun Xie (2016). Theoretical and Experimental Study on Electromechanical Coupling Properties of Multihammer Synchronous Vibration System. *Publishing Corporation Shock and Vibration*, Volume 2016, Article ID 6707264, 11 pages, <http://dx.doi.org/10.1155/2016/6707264>.

Nan Zhang, Shiling Wu (2020). Analysis of harmonic vibration synchronization for a nonlinear vibrating system with hysteresis force. *Journal of Low Frequency Noise, Vibration and Active Control*, Volume 39, Issue 4, 2020.

Yu Zhang, Luyu Li, Xiaohua Zhang (2017). Switch Control of Twin Rotor Damper for Bridge Vibration Mitigation under Different Excitations. *10th International Conference on Structural Dynamics*, EURO-DYN 2017, pp.1707-1712.

Jimin Zhao, Miao Xi (2020). Self-Tuning of PID Parameters Based on Adaptive Genetic Algorithm. *IOP Conference Series: Materials Science and Engineering*, Volume 782 (2020) 042028, DOI:10.1088/1757-899X/782/4/042028.

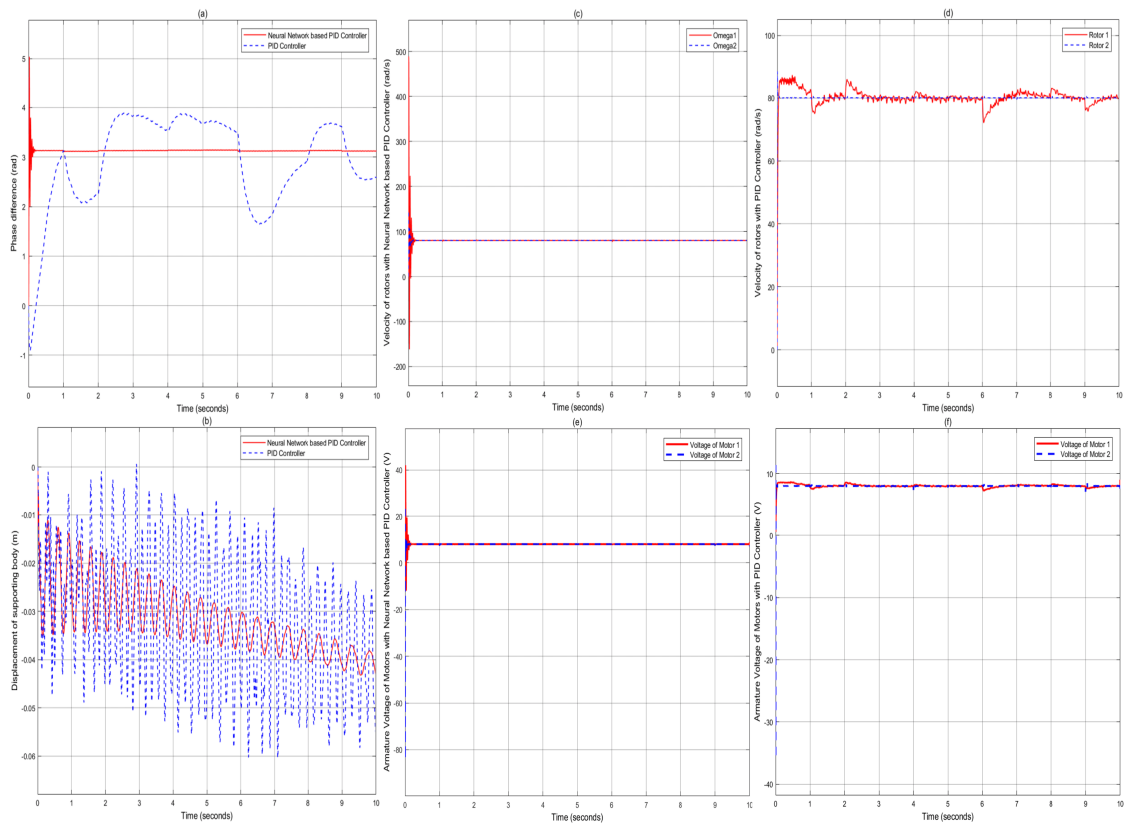


Figure 12. The response of system with change of the load.